

## Detection of Osteocalcin in Serum Based on Electrochemical Sensing Technology

Lanfang Lv<sup>1</sup>, Yehua Zhang<sup>2</sup>, Zongjiu Jiao<sup>2</sup> and Fang Cheng<sup>1,\*</sup>

<sup>1</sup> Department of Dermatology, Xingtai People's Hospital, Xingtai, Hebei, China 054000

<sup>2</sup> Department of Hematology, Xingtai People's Hospital, Xingtai City, Hebei Province, China 054000

\*E-mail: [chengfang20200925@163.com](mailto:chengfang20200925@163.com)

Received: 6 May 2022 / Accepted: 28 June 2022 / Published: 10 September 2022

---

Osteocalcin is a very useful potential biomarker to be used in the evaluation of multiple myeloma. This work constructs a competitive electrochemical immunosensor that enables the optimization and reapplication of osteocalcin direct competition ELISA at the electrode interface. Glutaraldehyde is commonly used as a bifunctional reagent. The two aldehyde groups within its structure can form Schiff bonds with the amino groups on the protein surface, which can enhance the interfacial adsorption and improve the interfacial binding of immobilized encapsulants. The present work was carried out by electrochemical methods. In this work, bovine serum albumin-osteocalcin immobilized antigen was used as the recognition element at the glassy carbon electrode interface, while osteocalcin antibody was added with the osteocalcin to be measured, and finally the antibody capture at the modified interface was determined by electrochemical methods. The signal sensitivity of this sensor is higher than that of ELISA, because of it eliminating the recombination process of the enzyme-labeled secondary antibody and theoretically reducing the possibility of introducing errors. The sensor provides linear detection of osteocalcin in the range of 2.0 ng/mL ~ 1250 ng/mL with a detection limit of 2.0 ng/mL. The sensitivity and stability of this sensor are excellent, and the established method can detect osteocalcin in real samples.

---

**Keywords:** Electrochemical sensor; Osteocalcin; Immunosorbent assay; Glutaraldehyde; Specific recognition

### 1. INTRODUCTION

Multiple myeloma is a malignant clonal disease in which plasma cells proliferate abnormally. Due to the interaction between myeloma cells and bone marrow microenvironment, infiltration of myeloma cells and their products, patients show clinical symptoms such as bone destruction, anemia and renal function impairment [1,2]. In the last decade, several biochemical markers of serum and urine for the evaluation of bone metabolism have been used in a large number of clinical trials for their low cost

and clinical usefulness. They can dynamically reflect the overall bone turnover rate and are clinically important for diagnosing, typing metabolic bone disease, predicting the risk of bone loss and fracture, and monitoring drug efficacy [3–5]. For multiple myeloma, bone metabolic markers provide a rapid, accurate, and dynamic picture of a patient's bone metabolic status. These indicators can help the clinic understand the extent of osteolytic damage in patients and give a reasonable treatment plan in time [6]. Serum osteocalcin is a vitamin K-dependent non-collagenous protein specifically synthesized and secreted by mature osteoblasts, adult dentin cells and hypertrophic chondrocytes [7]. Its synthesis is co-regulated by vitamin D and vitamin K. Osteocalcin is abundant in bone tissue, accounting for 15-20% of the non-collagenous protein of the bone matrix. The physiological role of osteocalcin is not fully understood, but it is known to be related to the rate of bone mineralization [8]. Osteocalcin, which is matured by carboxylation, is secreted out of osteoblasts and deposited in the bone matrix, with a small portion entering the blood circulation. When the bone matrix is degraded the osteocalcin in it enters the circulation [9,10]. Therefore, the measurement of osteocalcin in blood reflects the activity of osteoblasts and the status of bone transformation.

Currently, the established and widely used methods for the detection of osteocalcin are physicochemical and immunological assays [11,12]. These methods are highly sensitive and stable, but are usually costly and time-consuming. In order to meet the demand for rapid and efficient detection, new techniques for osteocalcin detection have been developed in recent years [13–21], among which the combination of immunological analysis and electrochemical methods can achieve trace analysis. The electrochemical immunosensor is an electrochemical detection method based on the immune reaction in ELISA as the analytical basis. It immobilizes the element to be recognized (antigen or antibody) at the electrode interface and determines the final state of the interface by step-by-step modification and electrochemical scanning [22–25]. After the interface captures the identified element, the interface state is changed by electrochemical scanning and the redox reaction signal on the electrode surface is converted into an electrical signal. In this study, a competitive electrochemical immunosensor was developed and assembled based on ELISA method. This assay technique has a simple pre-treatment process, shorter assay time, and better method recovery and stability. It has a limit of detection (LOD) of 2.0 ng/mL and can be applied to actual sample analysis. The ideas of signal amplification, interface modification and condition optimization for the construction of electrochemical immunosensor in this experiment can be potentially used in the field of small molecule detection.

## 2. EXPERIMENTAL

### 2.1. Materials and instruments

Ethylenediaminetetraacetic acid (EDTA), NaCl, KCl,  $C_6H_8O_7$ ,  $Na_2HPO_4 \cdot 12H_2O$ ,  $K_2CO_3$ ,  $NaHCO_3$ ,  $K_3[Fe(CN)_6]$ ,  $K_4[Fe(CN)_6] \cdot 3H_2O$ , 3,3',5,5'-tetramethylbenzidine (TMB), glacial acetic acid, Tween 20, concentrated sulfuric acid and anhydrous ethanol were purchased from Sinopharm Chemical Reagent Co. The dry powder of PBS buffer was purchased from Beijing Solebro Technology Co. Osteocalcin and its monoclonal antibody (Ab) were purchased from Abcam Systems, Cambridge, UK.

37% formaldehyde solution (HCHO) was purchased from Shanghai Collings Reagent Co. Bovine serum albumin (BSA) and sheep anti-mouse IgG-HRP antibodies were purchased from Beijing BoaoSen Biotechnology Co. The dialysis bag (MwCO 8000-14000) was purchased from Beijing Solabao Technology Co. The 3 mm diameter glassy carbon disc electrode (CHI104), saturated glycolic electrode (CHI150), platinum wire counter electrode (CHI115), electrode holder and electrode polishing material were purchased from Shanghai Chenhua Instruments Co. The 96-well enzyme labeling plate was purchased from BBI Life Sciences Co.

## 2.2. Preparation of BSA-HCHO-osteocalcin

Weigh 0.5 mg of osteocalcin solid standard accurately in a 10 mL beaker, add 500  $\mu$ L of 1% aqueous acetic acid solution and stir well to dissolve. The pH of the above solution was adjusted to 5.0 with potassium carbonate (0.1 mol/L). Weigh 5.0 mg of BSA solid, dissolve in 1 mL of PBS (pH 7.4) solution, and mix well. Transfer the prepared osteocalcin solution to a 2 mL EP tube, add 500  $\mu$ L of BSA solution drop by drop and mix well. Add 190  $\mu$ L of 37% formaldehyde solution to the mixture drop by drop and shake for 72 h at 37  $^{\circ}$ C. The reaction solution was transferred to a dialysis bag and dialyzed in PBS solution at 4  $^{\circ}$ C for 72 h. The solution was changed every 8 h. The reaction solution was diluted 10 times and the remaining diluted solution was stored at -20  $^{\circ}$ C. The final reaction solution was collected and diluted 10 times, and an appropriate volume was taken for UV absorbance value determination.

## 2.3. BSA-HCHO-osteocalcin immunogenicity assay

Take one 96-well enzyme plate, add 200  $\mu$ L of 0.8% glutaraldehyde solution to each well, and pretreat the plate at 37  $^{\circ}$ C for 6 h. Add 300  $\mu$ L of plate wash solution to each well when washing the plate. The BSA-osteocalcin reaction solution was diluted 5000-fold and 15000-fold with PBS buffer, respectively. Add 100  $\mu$ L of BSA-osteocalcin (diluted 5000 times) to each well in column 1 and 100  $\mu$ L of BSA-osteocalcin (diluted 15000 times) to each well in column 2, and coat overnight at 4  $^{\circ}$ C. Each well was added 250  $\mu$ L of 5 % BSA aqueous solution and closed at 37  $^{\circ}$ C for 2 h. Anti-osteocalcin solution was diluted with PBS buffer in a 3-fold gradient. The dilutions were  $3 \times 10^3$ ,  $9 \times 10^3$ ,  $2.7 \times 10^4$ ,  $8.1 \times 10^4$ ,  $2.43 \times 10^5$ ,  $7.29 \times 10^5$ ,  $2.187 \times 10^6$  and  $6.561 \times 10^6$ , respectively. After dilution, add 100  $\mu$ L of antibody solution diluted 3000 times to each well in row 1 in descending order of dilution. Add 100  $\mu$ L of antibody solution diluted 9000 times to each well of row 2. The final wells in row 8 are each filled with 100  $\mu$ L of antibody solution diluted  $6.561 \times 10^6$  times. The plates were incubated at 37  $^{\circ}$ C for 2 h. Goat anti-mouse IgG-HRP was diluted 4000 times (PBS dilution) and 100  $\mu$ L was added to each well and incubated at 37  $^{\circ}$ C for 40 min. After complete color development, the reaction was terminated by adding 50  $\mu$ L of termination solution to each well, and the UV absorbance values of each well at 450 nm and 620 nm were recorded.

#### 2.4. Construction of electrochemical immunosensor with glutaraldehyde modified substrate

Firstly, the GCE bare electrode interface was blown dry with N<sub>2</sub>, and the electrode was incubated in 200 µL of 0.8% glutaraldehyde aqueous solution for 1 h to activate the GCE interface (denoted as GCE/glutaraldehyde). 7 µL of BSA-osteocalcin (5.0 µg/mL) was applied dropwise to the electrode interface and dried naturally (denoted as GCE/glutaraldehyde/BSA-osteocalcin). The modified interface was placed in 200 µL of 2% BSA solution and closed at 37 °C for 1 h. After each modification process, the electrode should be immersed in water for 10 min and washed twice by oscillation to achieve a clean interface (denoted as GCE/glutaraldehyde/BSA-osteocalcin/BSA). Add 100 µL of osteocalcin standards (2, 10, 50, 250, 1250 µg/mL) with different concentration gradients to a 1.5 mL EP tube. After the interface is stabilized, 100 µL of anti-osteocalcin is added to each tube and incubated at 37 °C for 90 min. After incubation, the electrodes were removed and rinsed by soaking in water (denoted as GCE/glutaraldehyde/BSA-osteocalcin/BSA/anti-osteocalcin) for subsequent differential pulse voltammetry (DPV) scan detection. The scanning potential range was -0.4 V ~ 0.7 V. Cyclic voltammetry (CV) was used to characterize the changes in electrode properties after different modification steps with a scanning potential range of -0.3 V ~ 0.7 V and a scanning speed of 100 mV/s.

### 3. RESULTS AND DISCUSSION

Osteocalcin is a small molecule semi-antigen that is not immunogenic. Therefore, it cannot produce an immune response and cannot be used directly as an envelope. The usual approach is to obtain immunogenicity by selecting a suitable intermediate medium to couple small molecule semi-antigens to large molecule carrier proteins [26,27]. In general, the carrier proteins commonly used for small molecules are mostly BSA, keyhole limpet hemocyanin and ovalbumin. The osteocalcin structure contains guanidine groups within it. The Mannich reaction combines compounds containing active hydrogen with formaldehyde. The other end of the formaldehyde can be condensed with the exposed amino group at the protein end. Taking advantage of this property, formaldehyde can be chosen as an intermediate medium for the condensation reaction of the guanidine group of osteocalcin with the amino group of the carrier protein to achieve the synthesis of the complete antigen [28]. 10 µL of 1% BSA, 37% HCHO, osteocalcin (1.0 µg/mL) and BSA-HCHO-osteocalcin were pipetted onto the detection base of the ultra-micro UV-Vis spectrophotometer, and the specific results were detected as shown in Figure 1. The comparison revealed that BSA-HCHO-osteocalcin had more obvious absorption peaks of BSA and osteocalcin. The initial preparation of the artificial antigen was successful as evidenced by the blue shift near 280 nm. In order to further verify the immunogenicity of the artificial antigen [29], an ELISA method needs to be established for detection.

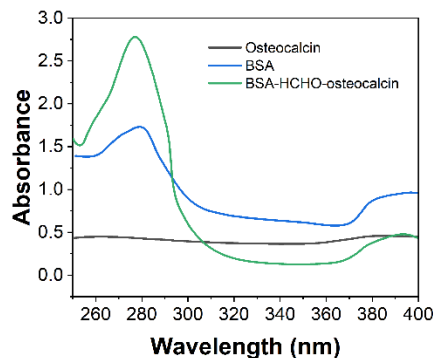


**Figure 1.** UV-vis spectra of osteocalcin, HCHO, BSA, BSA-HCHO-osteocalcin.

After the preparation of BSA-HCHO-osteocalcin (BSA-osteocalcin), the immunogenicity of the synthetic BSA-osteocalcin is determined on an enzyme-labeled plate to determine whether the synthetic BSA-osteocalcin specifically binds to anti-osteocalcin [30]. In the immunogenicity determination stage, the UV OD450 nm-OD620 nm of the final reaction wells prevailed, and the specific results are shown in Table 1. As the concentration of anti-osteocalcin decreases, the absorbance values of the corresponding reaction wells also decrease. The overall effect was better when BSA-osteocalcin was diluted 15000 times, which proved that the BSA-osteocalcin synthesized by this experiment had immunogenicity and could be used as a molecular probe for chemical modification at the electrode interface.

**Table 1.** Immunogenicity results of BSA-osteocalcin.

	<b>BSA-osteocalcin dilution ratio</b>	<b>5000</b>	<b>15000</b>
<b>Anti-osteocalcin dilution ratio</b>	3000	NA	3.745
	9000	NA	3.739
	27000	3.801	3.108
	81000	2.655	2.306
	243000	1.409	1.055
	729000	0.706	0.537
	2187000	0.373	0.283
	6561000	0.259	0.189

Figure 2 shows the scheme of preparation of electrochemical immunosensor for osteocalcin sensing. BSA is a commonly used containment reagent in immunological assays. It binds to non-specific recognition sites at the encapsulation interface and effectively prevents non-specific adsorption at subsequent immune reaction stages [31]. The level of blocking concentration affects the degree of binding of the antibody to the immobilized antigen. The presence of a very small amount of residual antibody in BSA may cause cross-reactivity or other side reactions between the residual antibody in BSA

and the interface-coated antigen, resulting in high background values or false positives [32,33]. On the contrary, a low concentration will not provide a sealing effect. In this experiment, 1%, 2% and 3% BSA were selected for the optimization of the closure phase. We determined the optimum concentration of confinement based on the percentage decrease in redox peak current before and after confinement. 50% was found to be the best choice. The current drop under 2% BSA closure was nearly 50%, so 2% BSA was chosen as the best closure solution.

The detection of this method is based on the establishment of an electrochemical scan of the final capture interface of the antibody, while the length of incubation time has a direct impact on the amount of antigen-antibody binding and the degree of reaction [34,35]. Therefore, the length of time that brings the antibody capture at the interface close to saturation and the reaction is adequate should be selected as the optimal incubation time. In this experiment, incubation times of 15 min, 30 min, 60 min, 90 min and 120 min were chosen to investigate the effect of specific reaction time on the sensor detection process. The peak current change ( $\Delta I$ ) of DPV before and after incubation reaches the highest point at 90 min, and the change of  $\Delta I$  is not obvious after 90 min, so 90 min should be selected as the best incubation time.

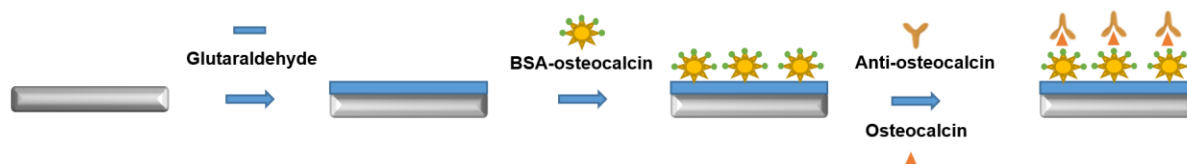


**Figure 2.** Scheme of preparation of electrochemical immunosensor for osteocalcin sensing.

To verify the validity of the modification process, the modification results need to be characterized for each step of the experimental operation [36]. We chose cyclic voltammetry (CV) to characterize the electrodes after each modification. As shown in Figure 3, the redox current of the GCE bare electrode starts to decrease after the modification of glutaraldehyde. The pending interfacial binding of BSA-osteocalcin impedes the rate of electron transfer at the electrode interface, resulting in a continued decrease in current. BSA is a macromolecular protein, and the whole is electrically neutral and cannot conduct electricity, and the surface reaction at the electrode interface is further hindered [37]. After binding of osteocalcin antibodies at the modified interface, the antigen-antibody complexes attach to the surface and affect the redox process of  $[\text{Fe}(\text{CN})_6]^{3-}$  and  $[\text{Fe}(\text{CN})_6]^{4-}$  at the interface-liquid interface. The characterization effect of each modification process is distinguished clearly and can prove that the modification is effective.

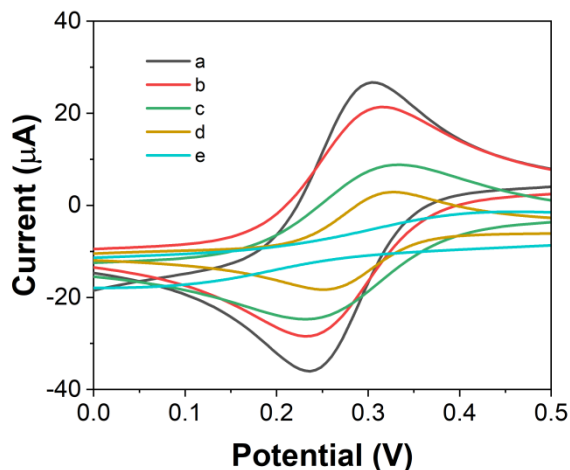


**Figure 3.** Cyclic voltammetry of osteocalcin electrochemical immunosensor on different preparation steps (a. Bare GCE; b. GCE/glutaraldehyde; c. GCE/glutaraldehyde/BSA-osteocalcin; d. GCE/glutaraldehyde/BSA-osteocalcin/BSA; e. GCE/glutaraldehyde/BSA-osteocalcin/BSA/anti-osteocalcin). Electrolyte: 2 mM  $[\text{Fe}(\text{CN})_6]^{3-/4-}$  (0.2 M KCl); Scan rate: 100 mV/s)

The effect of different concentrations of free osteocalcin in the solution on the binding process of antibodies can be seen from the competitive immunoconjugation method. The redox reaction rate at the electrode interface is then changed, and the detection result is finally reflected by the electrical signal obtained from the electrochemical scan [38,39]. As shown in Figure 4, osteocalcin concentration was positively correlated with  $\Delta I$ . The limit of detection can be calculated to be 1.17 ng/mL. The competitive mechanism involved can be explained as follows: The glutaraldehyde structure itself contains two aldehyde groups and functions as an intermediate at the interface between the semi-antigen and the solid phase. GCE interfacially modified glutaraldehyde may still react with and immobilize newly added osteocalcin after BSA blocking. The overall analytical performance of the GCE/glutaraldehyde/BSA-osteocalcin/BSA/anti-osteocalcin was compared with the previous literatures (see Table 2).

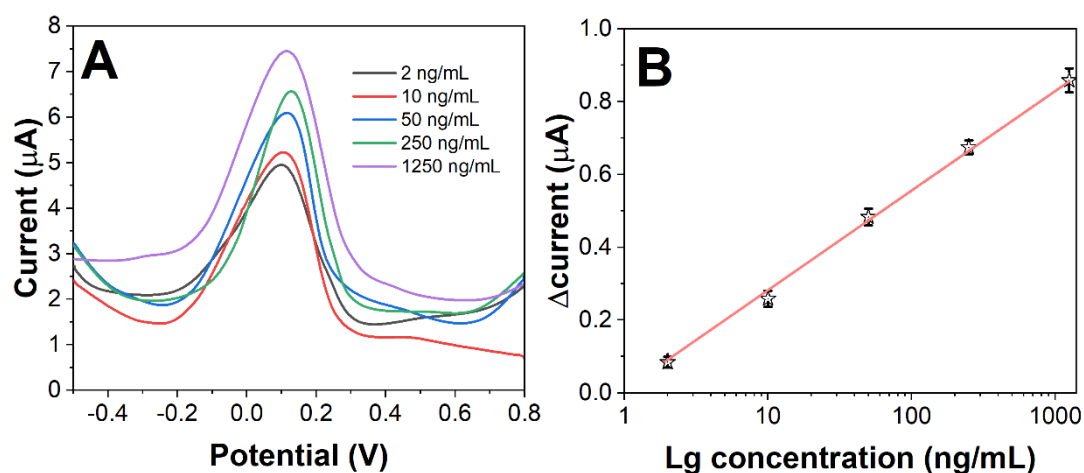


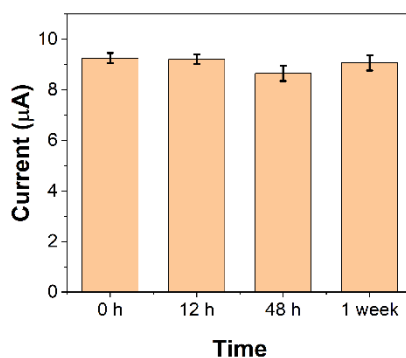
**Figure 4.** (A) DPV curves of GCE/glutaraldehyde/BSA-osteocalcin/BSA/anti-osteocalcin with 2 ng/mL, 10 ng/mL, 50 ng/mL, 250 ng/mL and 1250 ng/mL of osteocalcin. (B) Linearity between natural logarithm of osteocalcin concentration and DPV peak current variation ( $\Delta I$ ).

**Table 2.** Comparison of GCE/glutaraldehyde/BSA-osteocalcin /BSA/anti-osteocalcin with previously reported osteocalcin detection method.

Analytical method	Linear range	LOD	Reference
ELISA	-	0.13 ng/mL	[40]
ELISA	0.037-1.8 ng/mL	-	[41]
Antibody-Cu <sub>3</sub> (PO <sub>4</sub> ) <sub>2</sub> hybrid nanoflowers	0.1-50 ng/mL	0.042 ng/mL	[42]
ELISA assay	64.6-618.1 ng/mL	0.34 ng/mL	[43]
Current-volt sensor	0.01–3000 ng/mL	0.005 ng/mL	[44]
GCE/glutaraldehyde/BSA-osteocalcin /BSA/anti-osteocalcin	2-1250 ng/mL	1.17 ng/mL	This work

As the concentration of osteocalcin increases, the amount of interfacial fixation of osteocalcin increases and the amount of antibody capture at the modified interface subsequently increases, resulting in a higher  $\Delta I$  before and after incubation. The linear relationship between  $\Delta I$  and the natural logarithm of the osteocalcin concentration was  $y=0.124x+0.008$ ,  $r^2=0.998$ . The LOD of the method was 2.0 ng/mL ( $S/N > 3$ ).

The stability of the electrochemical immunosensor method is generally measured by the following three indicators [45]: the first is to test the stability of the sensing interface during the redox process by repeated cyclic scans of CV; the second is to calculate the relative stability of the detection results in parallel groups; and finally, the peak current is obtained by the DPV method at different times, and the stability of the sensor over a certain period of time is determined according to the current retention rate. The RSD was 2.21% for 20 cycles of the same sensor during CV scan. In addition to this, a parallel intra-group stability of 5.15% was calculated. Figure 5 reflects the degree of current retention of the immunosensor at 0 h, 12 h, 48 h and one week with an overall relative stability of 2.44%.

**Figure 5.** Peak current of GCE/glutaraldehyde/BSA-osteocalcin /BSA/anti-osteocalcin in different storage periods. Electrolyte: 2 mM [Fe(CN)<sub>6</sub>]<sup>3-/4-</sup> (0.2 M KCl); Scan rate: 100 mV/s)

A negative blank sample was selected, and 2.0  $\mu\text{g/mL}$  of osteocalcin standard solution was added before the pretreatment process. The final solution was spiked at a concentration of 50  $\text{ng/mL}$ , and an osteocalcin standard curve needed to be established to calculate the osteocalcin detection concentrations of the blank spiked samples based on the linear relationship, which was used to calculate the recovery. The results in Table 2 show that the overall recoveries ranged from 82% to 96%, proving that the method is accurate and feasible for actual sample detection.

**Table 2.** Recoveries of electrochemical immunosensor with the addition of osteocalcin.

Sample	Blank	1	2	3
$\Delta I$ ( $\mu\text{A}$ )	0.55	0.40	0.41	0.39
$\text{Ln}(c)$	0.34	3.78	3.90	3.73
$c$ ( $\text{ng/mL}$ )	1.43	44.68	49.5	42.2
Added ( $\text{ng/mL}$ )	-	50.00	50.00	50.00
Recovery (%)	-	86.66	95.97	82.42

In the actual sample analysis, we also use HPLC-MS to detect the samples. We performed detection with the proposed electrochemical immunosensor and compared the results with the detection by HPLC-MS (Table 3). The overall values detected by the sensor method were found to be smaller than those of HPLC-MS, but the difference was not significant. Such results suggest that the proposed electrochemical immunosensor can be practically used for the detection of osteocalcin.

**Table 3.** Comparison of detection of osteocalcin using proposed electrochemical immunosensor with traditional HPLC-MS.

Sample	Electrochemical immunosensor ( $\text{ng/mL}$ )	HPLC-MS ( $\text{ng/mL}$ )
1	74.15	76.21
2	135.02	144.03
3	194.22	197.51

#### 4. CONCLUSION

This work prepared the BSA-HCHO-osteocalcin complex and verified the immunogenicity of the complex. This complex can be specifically immunoconjugated on the basis of a 15,000-fold dilution of the reaction stock solution. Based on the ELISA competition analysis method, we fabricated an electrochemical immunosensing interface on glutaraldehyde substrate. The linear correlation between the natural logarithm of the sensor on osteocalcin concentration and the amount of change in DPV peak current before and after incubation was good in the range of 2.0  $\text{ng/mL}$  ~ 1250  $\text{ng/mL}$  ( $r^2 = 0.997$ ). LOD ( $S/N > 3$ ) was calculated to be 1.17  $\text{ng/mL}$ . The results of the methodological validation showed a high

immediate stability of the same sensor as well as a good stability within 1 week with an overall RSD below 3.0%. The accuracy of the method was further verified by the RSD of 5.15% for the detection results of the sensor within the same batch. The results of this method are highly accurate and consistent with those of HPLC-MS when applied to actual positive samples.

## References

1. Y. Feng, Y. Zhang, X. Wei, Q. Zhang, *Cancer Biomark.*, 24 (2019) 195–201.
2. J. Adamik, G.D. Roodman, D.L. Galson, *JBMR Plus*, 3 (2019) e10183.
3. Z. Liu, H. Liu, Y. Li, Q. Shao, J. Chen, J. Song, R. Fu, *J. Investig. Med.*, 68 (2020) 45–51.
4. C. Uhl, T. Nyirenda, D.S. Siegel, W.Y. Lee, J. Zilberberg, *Heliyon*, 8 (2022) e09167.
5. J. Adamik, D.L. Galson, G.D. Roodman, *J. Bone Oncol.*, 13 (2018) 62–70.
6. V. Béréziat, C. Mazurier, M. Auclair, N. Ferrand, S. Jolly, T. Marie, L. Kobari, I. Toillon, F. Delhommeau, B. Fève, *Cells*, 8 (2019) 441.
7. Y. Wu, Z. Zhang, J. Wu, J. Hou, G. Ding, *J. Healthc. Eng.*, 2022 (2022).
8. X. Wei, Q. Chen, Y. Fu, Q. Zhang, *J. Cell. Biochem.*, 120 (2019) 6515–6527.
9. C. Panaroni, K. Fulzele, T. Mori, C. Onyewadume, N.S. Raje, *Blood*, 136 (2020) 50.
10. S. Raimondo, O. Urzì, A. Conigliaro, G. Lo Bosco, S. Parisi, M. Carlisi, S. Siragusa, L. Raimondi, A. De Luca, G. Giavaresi, *Cancers*, 12 (2020) 449.
11. M. Chiu, D. Toscani, V. Marchica, G. Taurino, F. Costa, M.G. Bianchi, R. Andreoli, V. Franceschi, P. Storti, J. Burroughs-Garcia, *Cancers*, 12 (2020) 3267.
12. Z. Faraahi, M. Baud'huin, P. Croucher, C. Eaton, M. Lawson, *Bone*, 122 (2019) 82–92.
13. S. Han, Y. Xue, J. Zhang, J. Huang, X. Liu, Y. Yang, Z. Bai, C. Wang, *J. Anal. Methods Chem.*, 2020 (2020) 8891437.
14. B. Hu, Y. Liu, J. Deng, L. Mou, X. Jiang, *Anal. Methods*, 10 (2018) 2470–2480.
15. W. Pan, T. Jiang, T. Lu, Q. Jin, Y. Xi, W. Zhang, *Talanta*, 238 (2022) 123001.
16. H. Karimi-Maleh, Y. Orooji, F. Karimi, M. Alizadeh, M. Baghayeri, J. Rouhi, S. Tajik, H. Beitollahi, S. Agarwal, V.K. Gupta, *Biosens. Bioelectron.*, 184 (2021) 113252.
17. H. Karimi-Maleh, A. Khataee, F. Karimi, M. Baghayeri, L. Fu, J. Rouhi, C. Karaman, O. Karaman, R. Boukherroub, *Chemosphere*, 291 (2021) 132928.
18. H. Karimi-Maleh, F. Karimi, L. Fu, A.L. Sanati, M. Alizadeh, C. Karaman, Y. Orooji, *J. Hazard. Mater.*, 423 (2022) 127058.
19. H. Karimi-Maleh, M. Alizadeh, Y. Orooji, F. Karimi, M. Baghayeri, J. Rouhi, S. Tajik, H. Beitollahi, S. Agarwal, V.K. Gupta, S. Rajendran, S. Rostamnia, L. Fu, F. Saberi-Movahed, S. Malekmohammadi, *Ind. Eng. Chem. Res.*, 60 (2021) 816–823.
20. H. Karimi-Maleh, C. Karaman, O. Karaman, F. Karimi, Y. Vasseghian, L. Fu, M. Baghayeri, J. Rouhi, P. Senthil Kumar, P.-L. Show, S. Rajendran, A.L. Sanati, A. Mirabi, *J. Nanostructure Chem.*, 12 (2022) 429–439.
21. H. Karimi-Maleh, H. Beitollahi, P.S. Kumar, S. Tajik, P.M. Jahani, F. Karimi, C. Karaman, Y. Vasseghian, M. Baghayeri, J. Rouhi, *Food Chem. Toxicol.* (2022) 112961.
22. S.C. Moser, B.C. van der Eerden, *Front. Endocrinol.*, 9 (2019) 794.
23. M. Arponen, E.-C. Brockmann, R. Kiviranta, U. Lamminmäki, K.K. Ivaska, *Calcif. Tissue Int.*, 107 (2020) 529–542.
24. B. Joseph, M.A. Javali, M.A. Khader, S.M. AlQahtani, A. Mohammed, *Biomolecules*, 10 (2020) 380.
25. G.N. Eick, F.C. Madimenos, T.J. Cepon-Robins, M.J. Devlin, P. Kowal, L.S. Sugiyama, J.J. Snodgrass, *Am. J. Hum. Biol.*, 32 (2020) e23394.
26. P. Khashayar, G. Amoabediny, M. Hosseini, R. Verplancke, F. Razi, J. Vanfleteren, B. Larijani, *IEEE Sens. J.*, 17 (2017) 3367–3374.

27. Z.U. Rahman, W. Haider, L. Pompa, K. Deen, *Mater. Sci. Eng. C*, 58 (2016) 160–168.
28. K. Mustafa, J. Pan, J. Wroblewski, C. Leygraf, K. Arvidson, *J. Biomed. Mater. Res. Off. J. Soc. Biomater. Jpn. Soc. Biomater. Aust. Soc. Biomater. Korean Soc. Biomater.*, 59 (2002) 655–664.
29. Y. Mohamed Hassan, L. Massa, C. Caviglia, S. Sylvest Keller, *Electroanalysis*, 31 (2019) 256–266.
30. X. Jia, Y. Zhou, L. Tan, Q. Xie, H. Tang, M. Ma, S. Yao, *Electrochimica Acta*, 54 (2009) 3611–3617.
31. B. Chico, B.T. Pérez-Maceda, S. San-José, M.L. Escudero, M.C. García-Alonso, R.M. Lozano, *Materials*, 15 (2022) 2693.
32. C. Yao, V. Perla, J.L. McKenzie, E.B. Slamovich, T.J. Webster, *J. Biomed. Nanotechnol.*, 1 (2005) 68–73.
33. L. Xu, X. Yu, W. Chen, S. Zhang, J. Qiu, *RSC Adv.*, 10 (2020) 8198–8206.
34. W. Kim, H. Choe, Y. Ko, *J. Korean Inst. Surf. Eng.*, 41 (2008) 69–75.
35. M. García-Alonso, L. Saldana, G. Valles, J.L. González-Carrasco, J. Gonzalez-Cabrero, M. Martinez, E. Gil-Garay, L. Munuera, *Biomaterials*, 24 (2003) 19–26.
36. M. Liu, L. Hao, Q. Huang, D. Zhao, Q. Li, X. Cai, *J. Nanosci. Nanotechnol.*, 18 (2018) 3134–3140.
37. P. Venkatsurya, B. Girase, R. Misra, T. Pesacreta, M. Somani, L. Karjalainen, *Mater. Sci. Eng. C*, 32 (2012) 330–340.
38. H. Bhadracha, M.I. Khatkhatay, M. Desai, *Clin. Chim. Acta*, 489 (2019) 117–123.
39. A. Boudenot, S. Pallu, R. Uzbekov, E. Dolleans, H. Toumi, E. Lespessailles, *Appl. Physiol. Nutr. Metab.*, 46 (2021) 1525–1534.
40. S. Jiang, H.W. Cheng, P.Y. Hester, J.-F. Hou, *Poult. Sci.*, 92 (2013) 1951–1961.
41. J. Lacombe, O. Al Rifai, L. Loter, T. Moran, A.-F. Turcotte, T. Grenier-Larouche, A. Tchernof, L. Biertho, A.C. Carpentier, D. Prud'homme, R. Rabasa-Lhoret, G. Karsenty, C. Gagnon, W. Jiang, M. Ferron, *Am. J. Physiol.-Endocrinol. Metab.*, 318 (2020) E381–E391.
42. W. Pan, T. Jiang, T. Lu, Q. Jin, Y. Xi, W. Zhang, *Talanta*, 238 (2022) 123001.
43. G.N. Eick, F.C. Madimenos, T.J. Cepon-Robins, M.J. Devlin, P. Kowal, L.S. Sugiyama, J.J. Snodgrass, *Am. J. Hum. Biol.*, 32 (2020) e23394.
44. H. Bi, P. Bian, S.C.B. Gopinath, K. Marimuthu, G. Lv, X. Yin, *Biotechnol. Appl. Biochem.*, n/a (2021).
45. S.S. Hatkar, S.S. Kadam, M.I. Khatkhatay, M.P. Desai, *Indian J. Clin. Biochem.*, 35 (2020) 436–441.